DINAME 2019 - Proceedings of the XVIII International Symposium on Dynamic Problems of Mechanics,
M.A. Savi, T.G. Ritto and W.M. Bessa (Editors), ABCM, Buzios, RJ, Brazil, March 10th to 15th, 2019

DINAME 2019 – Behavior of Ultra High Performance Fiber Reinforced Concrete (UHPFRC) under seismic load

Rúbia M. Bosse [1], Gustavo de Miranda Saleme Gidrão[2], André Teófilo Beck [3], Ricardo Carrazedo [4]

[1] São Carlos School of Engineering, University of São Paulo, Brazil, rubiabosse@usb.br,

[2] São Carlos School of Engineering, University of São Paulo, Brazil, gustavo.gidrao@usp.br,

[3] São Carlos School of Engineering, University of São Paulo, Brazil, atbeck@usp.br.

[4] São Carlos School of Engineering, University of São Paulo, Brazil, carrazedo@usp.br.

Abstract: Ultra-high performance fiber-reinforced concrete (UHPFRC) is a new material with unique mechanical properties as well as high ductility and toughness which makes it a promising material for use in earthquake-resistant structures. This paper addresses the response of a 4-storey frame model with solid finite elements method and composed by reinforced concrete subjected to the El Centro earthquake ground displacements. The dynamical response of the structure of UHPFRC is compared to the response of the same structure made by a conventional high strength concrete. The mechanical model describes physical nonlinear behavior with damage and plasticity showing the regions of cracking propagation. UHPFRC presented smaller levels of damage in all time instants and higher equals displacements for floors compared with the response of the conventional high strength concrete. The material showed ductile behavior and capacity to inhibit the crack propagation.

Keywords: Ultra-high performance fiber-reinforced concrete, physical nonlinear behavior, dynamical response, earthquake-resistant structures.

INTRODUCTION

Ultra-high performance fiber-reinforced concrete (UHPFRC) is a new material that presents unique mechanical properties to Civil Engineering Industry. UHPFRC is usually composed by usual cement, silica powder, superplasticizers, small percentage of water and high strength metallic fibers. The combination of optimum mix proportions with controlled production conditions ensures high compressive strength (up to 130 MPa), high durability, low permeability and satisfactory ductile behavior. Due to these properties, UHPFRC is suitable to seismic resistant structures.

Concretes with high performance are characterized by low water-cement ratio (w/c = 0,2) and minimal compressive strength at 28 days of 150 MPa. However, with the increase of strength and decrease in microstructure imperfections, the material can present a fragile rupture. To deal with this limitation, steel fibers with high strength (2850 MPa in tension) are added to the mixture. It is relevant to emphasize that the addiction of metallic fibers does not dispense the use of reinforcements in design (Russel and Graybeal, 2013; Wang et al, 2015; Graybeal, 2014).

There are many recent papers dealing the performance of UHPFRC in diverse backgrounds including seismic resistant structures. Xu et al. (2018) studied the behavior of steel frames with UHPC joints and friction damper applied to beam-column connections under seismic loads. Mohebbi et al. (2018) performed a shaking table test in a large-scale precast bridge column and used ultra-high concrete to mitigate seismic damage in the connection between the column base and the precast footing (with pocket connection), results showed that the connection was effective to form a plastic hinge in the column without damage. The use of UHPC enhanced the performance to buckling and eliminated the effects of low-cycle fatigue failure.

This paper addresses the response of UHPFRC under seismic loads and investigates the robustness of the material for prevent damage evolution. The dynamic analysis of a 4-storey frame subjected to *El Centro* earthquake is performed through a finite elements model with ABAQUS CAE®. The dynamic response of the structure composed by a conventional high strength concrete (C70) is compared to the response of UHPFRC building.

A refined constitutive model of damage coupled with plasticity (i.e. Concrete Damage Plasticity) is used to represent the behavior of the concrete in the structure. Solid 3D finite elements were used to represent the concrete material, steel reinforcements were totally embedded in concrete. Earthquake ground displacements are applied to the base of columns to simulate realistically the occurrence of a seismic event.

The results of qualitative evolution of damage showed that concrete C70 present damage and cracking in the beginning of the analysis with high concentration of damage in the first connection column-beam. UHPFRC building,

showed a smaller rate of damage evolution in time and capacity to inhibit the crack propagation in the beginning of the analysis compared to C70 response.

Mechanical Model

Mehta and Monteiro (2008), show that, besides the behavior of the components of concrete (aggregate and paste) isolated present a linear stress-strain diagram, its combination in the mixture presents nonlinear tendency. This behavior can be explained by the previous microcracking in the interfacial transition zone and by the differences in the elastic properties of the components. In this way, the parcels of stiffness degradation and plastic strain have to be taking into account to precisely represent concrete structures.

Concrete Damage Plasticity

The Concrete Damage Plasticity (CDP) is a model already implemented in ABAQUS CAE®. It describes the behavior of concrete in a predetermined stress state, coupling the concepts of plasticity and damage (Johnson, 2006; Wahalathantri et al., 2011, Jankowiak and Lodygowski, 2005). The model admitts two failure mechanisms: (i) tension rupture and (ii) compression crushing. Figure 1 presents the tensive and compressive uniaxial responses of concrete, in CDP.

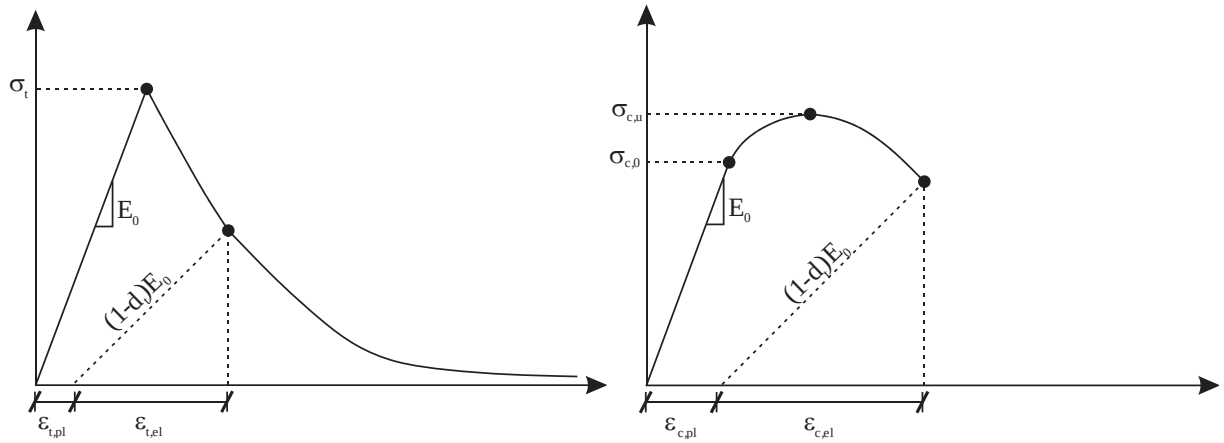

a) uniaxial traction **b) uniaxial compression**

Figure 1 – Uniaxial stress-strain response of concrete.

$\varepsilon_{t,pl}$ and $\varepsilon_{c,pl}$ are the plastic strains in traction and compression; $\varepsilon_{t,el}$ $\varepsilon_{c,el}$ are the elastic strains in traction and compression; E_0 is the initial elasticity modulus; d is the damage index; σ_t is the maxim traction stress and its respective elasticity limit; $\sigma_{c,0}$ is the limit of elasticity for uniaxial comprresion; $\sigma_{c,u}$ is the maxim compressive stress.

It can be stablished a constituve law to correlate Cauchy tensor of stress (σ) to the tensors of strains (ε e ε_{pl}):

$$\sigma = (1-\mathrm{d})\,\mathrm{E}_0 : (\varepsilon - \varepsilon^{pl}) = \mathrm{E}_{el} : (\varepsilon - \varepsilon^{pl}) \tag{1}$$

Where, d is the damage index; ε is the tensor of total strains; ε_{pl} is the tensor of plastic strains; E_{el} is the damaged elastic stiffness, given by: $E_{el}=(1\text{-}d)E_{0;}$ (ε -ε_{pl}) are defined as the inelastic strain. All analysis performed in this paper adopted CDP model to represent the nonlinear behavior of concrete.

STUDIED CASE

A 4-storey frame with 12 meters high is subjected to *El Centro* Earthquake ground displacements. Beams are 7.6 meters long and have cross section of 40 x 40 cm. Columns are 3 meters high and have rectangular (20 x 20 cm) cross section. The structure was discretized with solid C3D8 elements (Fig. 2.a). The elements are reinforced with longitudinal and transversal by steel bars. The reinforcements are modelled with 3-D truss elements T3D2 element (Fig. 2.b) totally embedded within the concrete (Fig. 2.c). The mesh is divided each 0.1 meters for concrete and longitudinal bars, each 0.05 meters for stirrups. A more refined mesh is applied to the connection regions, where it is expected higher damage levels (Fig. 3). Stirrups have 3 cm²/m area, representing bars with f = 6.3mm placed each 20cm, longitudinal reinforcement has 4.91 cm² area (4 f 12.5 mm). The density of concrete and steel are 2500 kg/m³ and 7500 kg/m³, in order. The dynamic response of the frame is evaluated when composed by a usual high strength concrete (C70, i.e. 70MPa compressive strength) and UHPFRC (with 145MPa compressive strength).

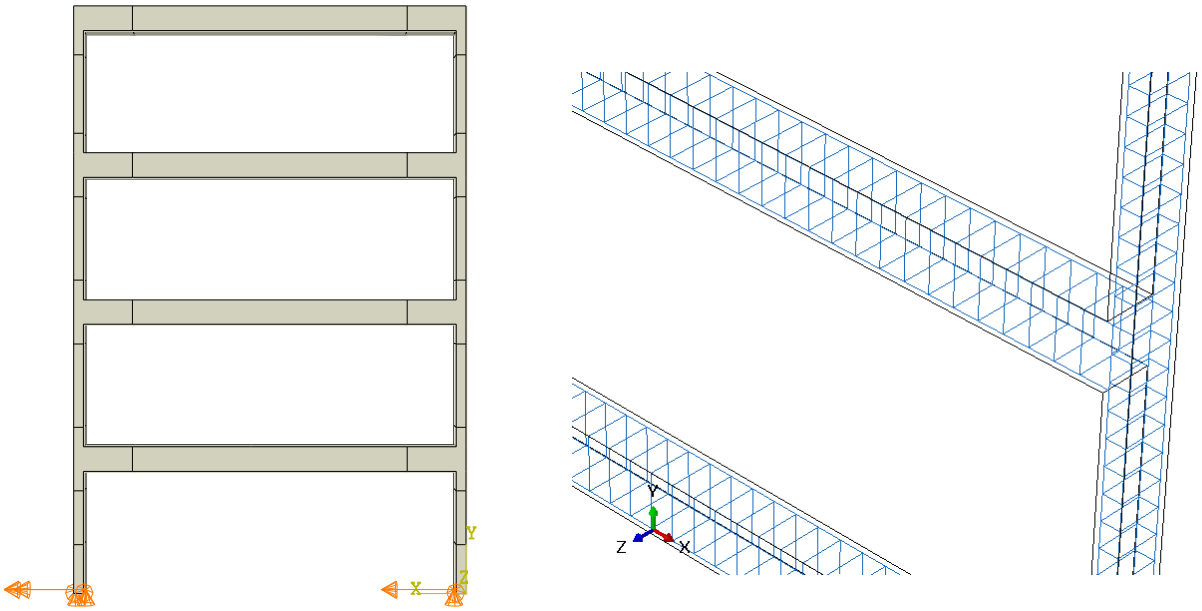

(a) **(b)**

Figure 2 – a) displacements application point; b) Steel reinforcements embedded in concrete.

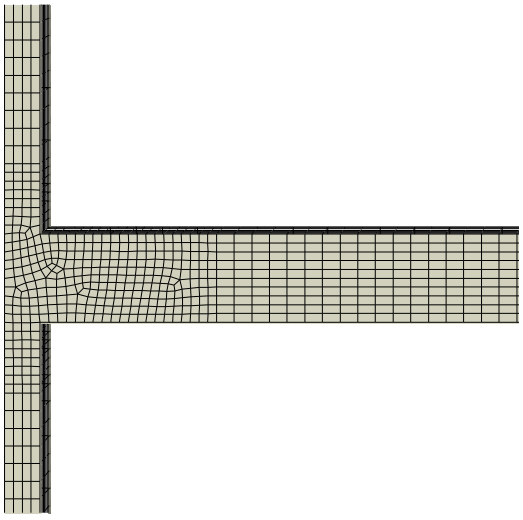

Figure 3 – Joint refined mesh zones.

Dead loads are considered for all elements (with g = -9,81m/s²). The building is subjected *El Centro* earthquake displacements during 25 seconds. Displacements of *El Centro* (Fig. 3.a) were obtained through a record of the acceleration signal. A delay of 0.02 seconds in ground displacements was considered between columns.

Figure 4 and 5 present the constitutive law of concretes. Figures 4.a and b present the behavior of UHPFRC, produced by Krahl et. al (2018.a) and Krahl et. al (2018.b). Figure 5.a and b present constitutive relation for C70, obtained by analytical indications of CEB FIB 2010. Any dynamic increase factor was considered in favour of safety. The constitutive model of steel is considered as perfectly plastic with yield stress equal to 500MPa. A compressive recovery of 100% was considered in models and the tensile recovery was disregarded, in favour of safety. Steel fibers were considered in the constitutive law of UHPFRC. Table 1 presents the properties of materials and Table 2 presents the concrete plasticity properties.

It is relevant to emphasize that the computation costs of this type of analysis can be demanding in the study. For the analysis of this structure under 25 seconds of earthquake, about 30 hours processing were spent, using four processors in parallel.

Table 1 – Elastic properties of materials

Material	E_0 (GPa)	Compressive Strength (MPa)	Tensile Strength (MPa)
C70	50.0	70.0	4.40
UHPFRC	55.0	145.0	7.0
Steel CA50	210.0	-*	-*

*the rupture of reinforcements was not considered in the model

Table 2 – Plastic properties of Concrete

Material	Dilation angle (º)	Eccentricity	f_{bo}/f_{co}	K	Visc.
C70	54	0.1	1.05	0.666	0.0001
UHPFRC	54	0.1	1.05	0.666	0.0001

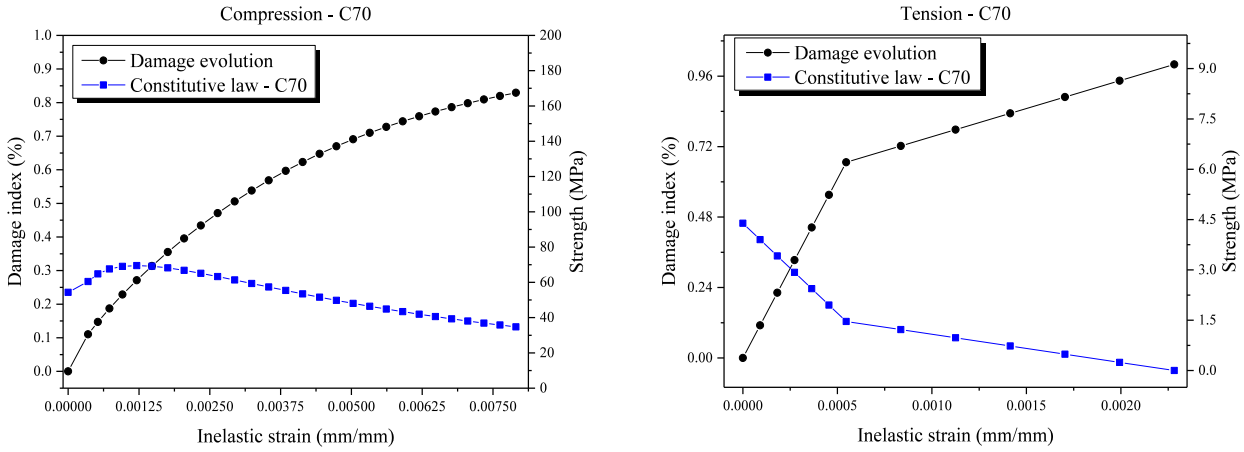

Figure 4 – Constitutive law and damage evolution of C70

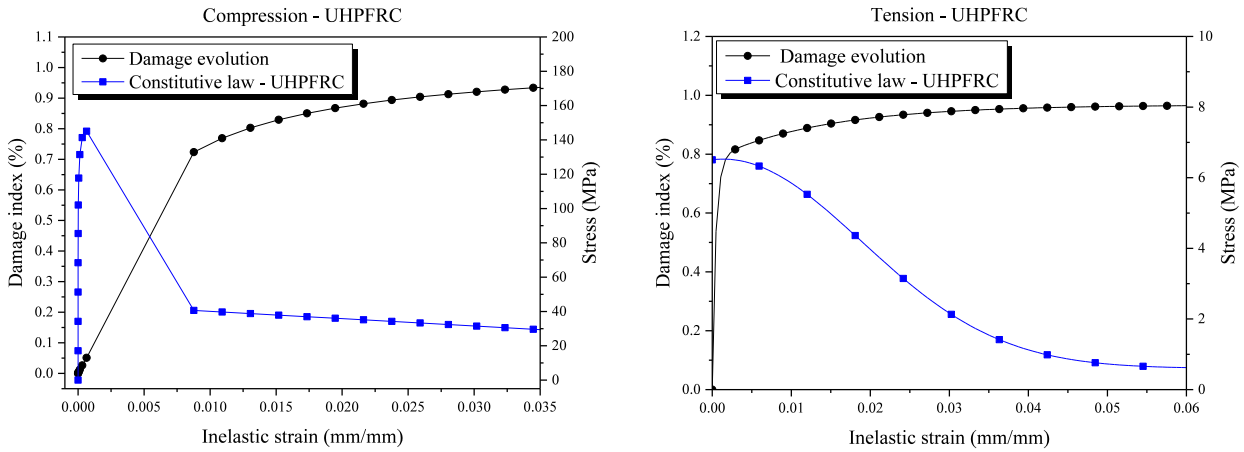

Figure 5 – Constitutive law and damage evolution of UHPFRC.

RESULTS

Figure 6 presents the top displacements in the last floor for the structure made of C70 and UHPFRC and compare this to base displacement:

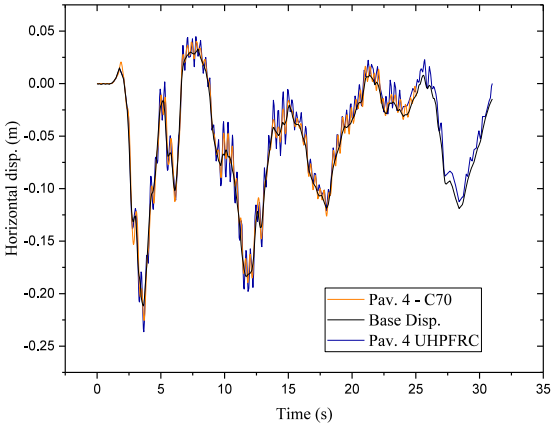

Figure 6 – Top and base horizontal displacements of C70 and UHPFRC structures

UHPFRC and C70 displacements were similar during the Earthquake, reaching maximum positional displacement of 25 cm at 4.75 seconds.

Figures 7 and 8 present the tensile damage at 5 and 20 seconds of analysis for the structure made of C70 and UHPFRC.

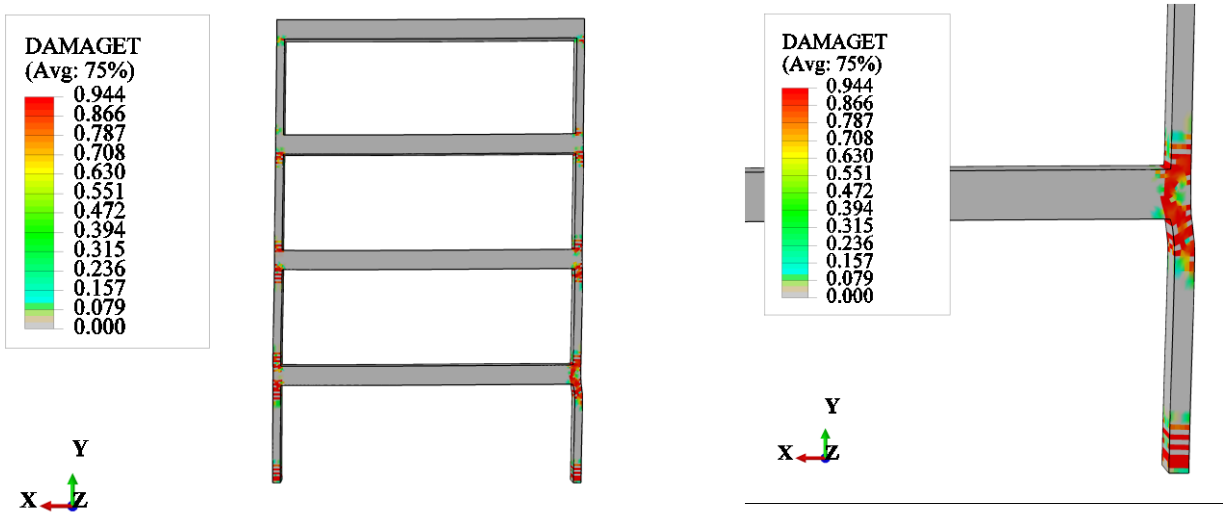

(a) C70 **(b) C70**

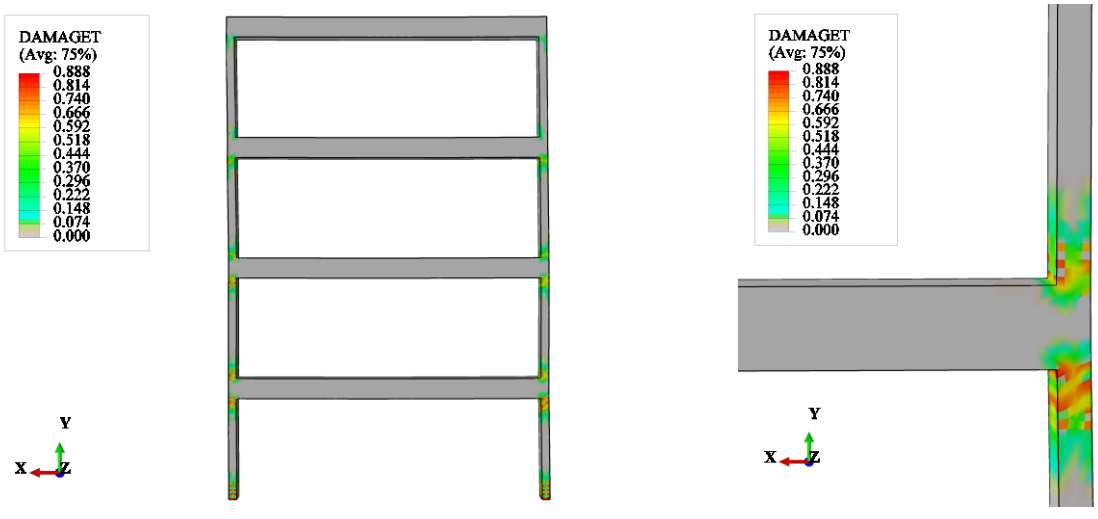

(c) UHPFRC **(d) UHPFRC**

Figure 7 – Tensile Damage in 5 seconds of analysis for C70 (a) and (b) and UHPFRC (c) and (d).

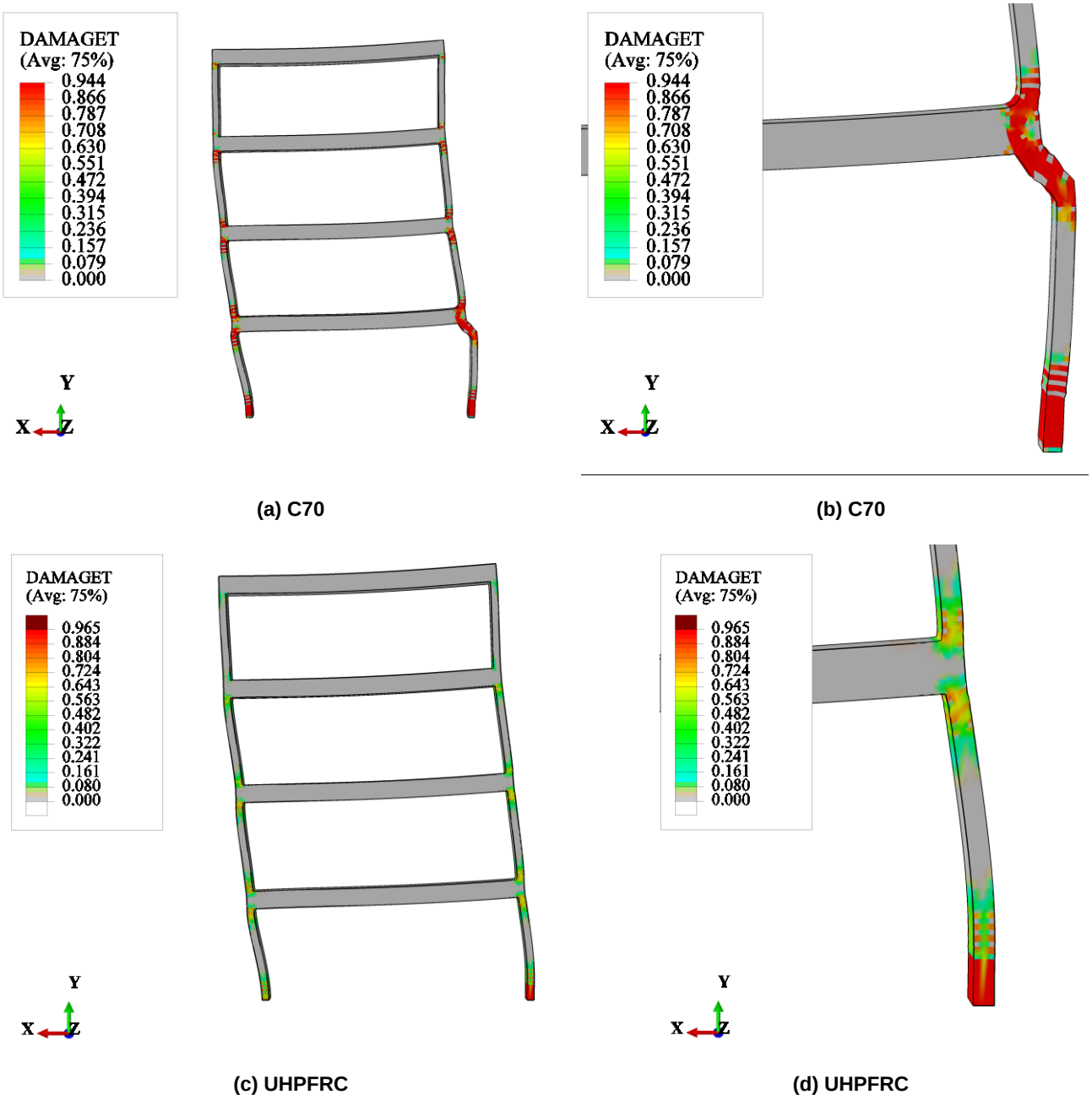

(a) C70 **(b) C70**

(c) UHPFRC **(d) UHPFRC**

Figure 8 – Tensile Damage at 20 seconds of analysis for C70 and UHPFRC.

Figures 7 and 8 showed the concentration of damaged zones in the beam-column connections indicating the formation of plastic hinges, as expected. It can be verified that C70 structure presents high cracking level in the beginning of analysis (i.e. 5 seconds), mainly in first floor joint and in the base of one column with a wide damaged region. At 20 seconds C70 frame shows already signals of failure in the base of column and in first floor connection with damage levels around 95% and visible distortions in elements.

UHPFRC structure shows more controlled damage propagation in joints, around 60%. The structural failure indicated in Fig. 8.d) occurs in the base of column. This same concentration of damage can be verified in the base of the columns of both models, and can be attributed to the modeling assumptions, where a proper foundation element was not applied.

Figure 9 presents the comparison of the mean tensile damage index found in all connection refined regions (Fig. 3) for the structure with C70 and UHPFRC.

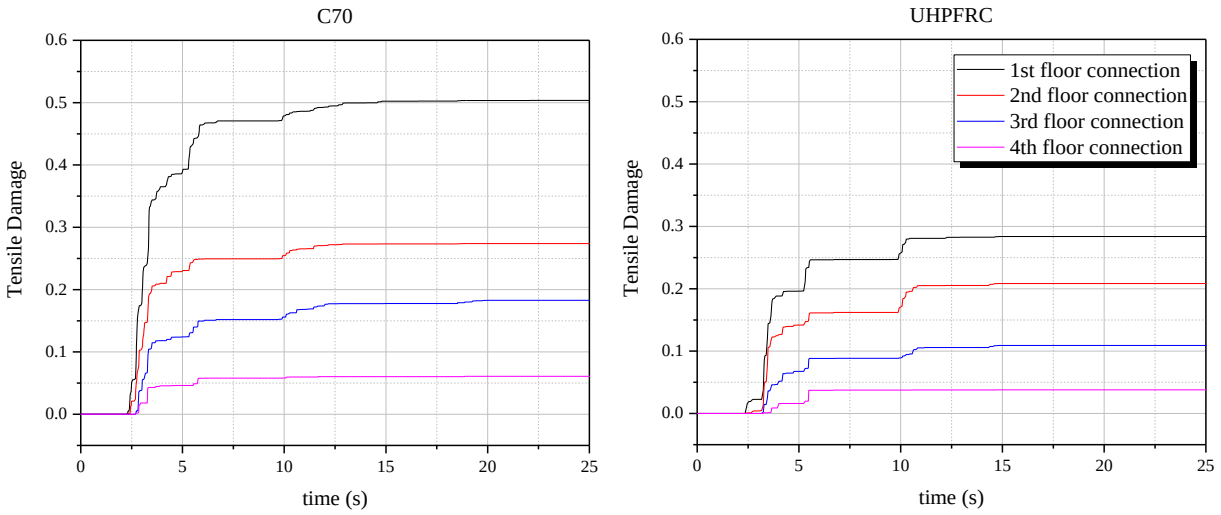

Figure 9 – Evolution of tensile damage in each floor connection over time for C70 and UHPFRC strutures.

In both models the damage index in the 1st floor connection is higher than in the other connections. The mean damage indexes found for UHPFRC were around 50% smaller than C70 ones, showing that the material inhibits the damage propagation compared to the conventional high strength concrete.

Figure 10 present the stress of steel reinforcements of the first floor column-beam connection for the frame composed by C70 and UHPFRC at 12 seconds of analysis. Figure 11 presents the maxim envelope Von Mises stress of reinforcements in this same joint along all analysis time.

Figures 10 and 11 indicated that the maxim stress in C70 structure reaches near values of 500MPa, the yield stress for CA50 steel. UHPFRC mean maxim stress was around 350MPa, showing a decrease about 30% in the stress of the bars and the effectiveness of steel alleviating the stress in reinforcement. After 2.5 seconds the damage increases severally in both material, what causes major requests in reinforcements (see Figs. 7, 8 and 9).

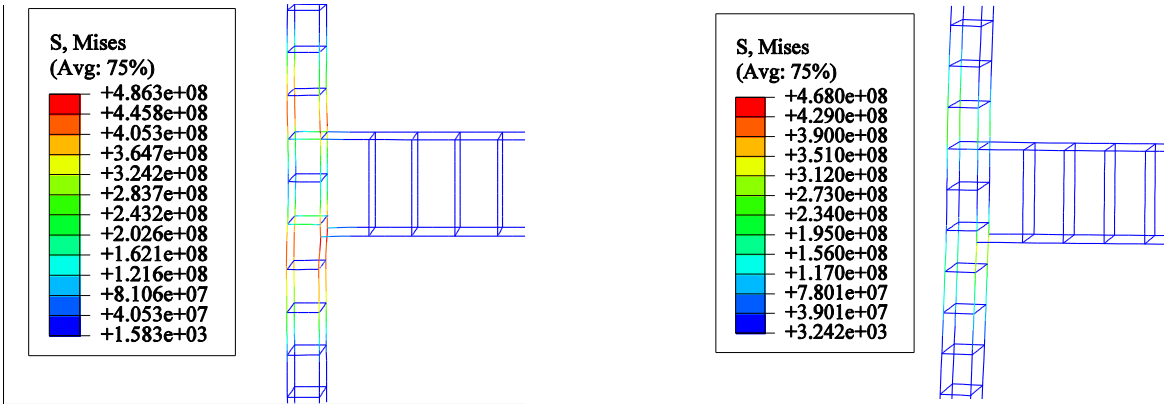

(a) C70 **(b) UHPFRC**

Figure 10 – Strength in the reinforcements at 12 seconds.

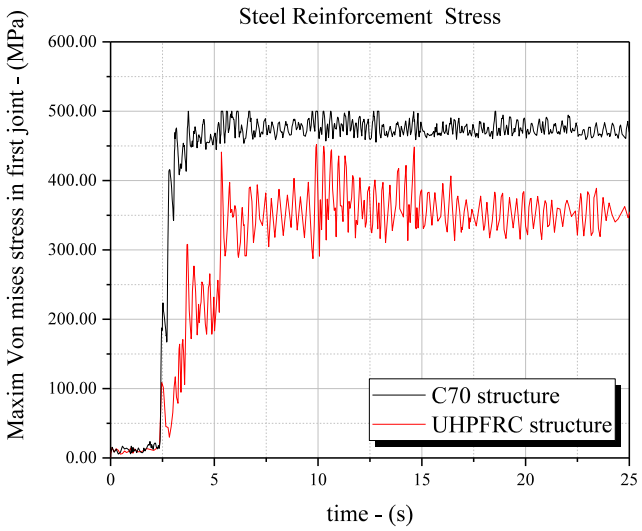

Figure 11 – Strength of steel reinforcements in time in the joint region.

CONCLUDING REMARKS

The paper focused in the dynamic response of a 4-storey frame composed by C70 (usual high strength concrete) and UHPFRC (Ultra High Performance Fiber Reinforced Concrete) with steel reinforcements, subjected to *El Centro* earthquake. A 3D solid finite elements model was developed in ABAQUS SIMULIA CAE, accounting with physical nonlinear analysis using Concrete Damage Plasticity and plasticity for reinforcement bars. The earthquake was simulated as ground horizontal displacements applied to the base of columns, and results of damage index, top displacements and stress in steel were evaluated.

Following aspects were remarkable:

1) As expected the tensile damage was concentrated in joints, indicating the formation of plastic hinges. The damage indexes decreases with the height of the building, showing higher values in the first connection;
2) For same imposed base displacement, UHPFRC showed small levels of cracking in all time instant for all connections, mean response about 50% smaller than C70 damage indexes;
3) UHPFRC alleviated the stress in reinforcement in 30 %;
4) Steel reinforcements of UHPFRC did not showed plastic strains;
5) Both structure showed signals of failure due to the shear force in the constraints, a more refined model considering the foundation elements should be applied to increase the strength of the base column.

ACKNOWLEDGMENTS (HEADING 1, HELVETICA 11PT BOLD ALL CAPS)

The authors gratefully acknowledge the financial support provided by National Counsel of Technological and Scientific Development (CNPq).

REFERENCES

CEB FIB, 2010 – “Model Code 2010”.

Graybeal, B. A., 2008, “Flexural Behavior of an Ultrahigh-Performance Concrete I-Girder,” J. Bridg. Eng. 13 602–610. doi:10.1061/(ASCE)1084-0702(2008)13:6(602).

Graybeal, B. A., Baby, F., 2010, “Development of Direct Tension Test Method for Ultra-High-Performance Fiber-Reinforced Concrete”, ACI Mater. J. 177–186. doi:10.14359/51685532.

Jankowiak, T.; lodygowski, T., 2005, “Identification of parameters of concrete damage plasticity constitutive model”. Foundations of civil and environmental., n. 6, p. 53–69.

Krahl, P.A., Gidrão, G. M. S., Carrazedo, R., 2018, “Compressive behavior of UHPFRC under quasi-static and seismic strain rates considering the effect of fiber content”, Constr. Build. Mater. 188 633–644. doi:10.1016/j.conbuildmat.2018.08.121.

Krahl, P.A., Carrazedo, R., El Debs, M.K., 2018, “Mechanical damage evolution in UHPFRC: Experimental and numerical investigation”, Eng. Struct. 170 doi:10.1016/j.engstruct.2018.05.064.

Mehta, P. K., Monteiro, P. J. M., 2005, "Concrete – Microstructure, Properties and Materials", McGraw-Hill, Third Edition.

Russel, H., G, Graybeal, B. A, 2013, "Ultra-High Performance Concrete : A State-of-the-Art Report for the Bridge Community".

Wahalathantri, B. L.; thambiratnam, D.; chan, T.; Fawzia, S., 2011, "A material model for flexural crack simulation in reinforced concrete elements using ABAQUS". Proceedings of the First International Conference on Engineering, Designing and Developing the Built Environment for Sustainable Wellbeing.

Wang, D., Shi, C., Wu, Z. J. Xiao, Huang, Z., 2015, "Fang, A review on ultra-high performance concrete : Part II . Hydration , microstructure and properties," Constr. Build. Mater. 96 368–377. doi:10.1016/j.conbuildmat.2015.08.095.

Jankowiak, T, and T Lodygowski. 2005. "Identification of Parameters of Concrete Damage Plasticity Constitutive Model." Foundations of civil and environmental … (6): 53–69.

Johnson, S. 2006. "Comparison of Nonlinear Finite Element Modeling Tools for Structural Concrete." University of Illinois.

Mohebbi, Alireza et al. 2018. "Shake Table Studies and Analysis of a PT-UHPC Bridge Column with Pocket Connection." 144(4).

Ozbakkaloglu, Togay, and Murat Saatcioglu. 2007. "Seismic Performance of Square High-Strength Concrete Columns in FRP Stay-in-Place Formwork." Journal of Structural Engineering 133(January): 44–56.

Wahalathantri, Buddhi L., D. Thambiratnam, T. Chan, and S. Fawzia. 2011. "A Material Model for Flexural Crack Simulation in Reinforced Concrete Elements Using ABAQUS." Proceedings of the First International Conference on Engineering, Designing and Developing the Built Environment for Sustainable Wellbeing.

Xu, Tengfei, Di Zheng, Cheng Yang, and Kailai Deng. 2018. "Seismic Performance Evaluation of Damage Tolerant Steel Frame with Composite Steel-UHPC Joint." Journal of Constructional Steel Research 148: 457–68.

RESPONSIBILITY NOTICE

The authors are the only responsible for the printed material included in this paper.